DOI:10.1021/jf9036722

JOURNAL OF AGRICULTURAL AND FOOD CHEMISTRY
ARTICLE

Spectral Alteration and Degradation of Cyanidin-3-glucoside Exposed to Pulsed Electric Field

Yan Zhang, Jianxia Sun, Xiaosong Hu, and Xiaojun Liao*

College of Food Science and Nutritional Engineering, China Agricultural University, Key Laboratory of Fruits and Vegetables Processing, Ministry of Agriculture, Engineering Research Centre for Fruits and Vegetables Processing, Ministry of Education, Beijing 100083, China

Anthocyanins are polyphenol antioxidants that have been shown to prevent many chronic diseases. The compounds are not stable, so they tend to be decolorized or degraded during processing and storage. In this study, the spectral characteristics alteration and degradation products of cyanidin-3-glucoside (Cyd-3-glc) exposed to pulsed electric field (PEF) were investigated, and the reaction kinetics was discussed. The intensity of the UV−vis spectra decreased noticeably upon PEF treatment without modification of the spectral pattern. Protocatechuic acid and 2,4,6-trihydroxybenzoic acid were identified as degradation products of both PEF and thermally treated Cyd-3-glc, but cyanidin present in thermally treated Cyd-3-glc was absent in PEF-treated Cyd-3-glc, indicating that the first step of Cyd-3-glc degradation induced by PEF was not the hydrolysis of glycosidic bonds, which was different from that of thermal degradation. With increased electric field intensity or treatment time, the degradation of Cyd-3-glc and the formation of protocatechuic acid were enhanced; their kinetics (except 7 kV/cm for protocatechuic acid formation) were well fitted to a first-order reaction. Meanwhile, a good correlation was present between Cyd-3-glc degradation and protocatechuic acid formation.

KEYWORDS: Cyanidin-3-glucoside; pulsed electric field; kinetics; protocatechuic acid; 2,4,6-trihydroxybenzoic acid

INTRODUCTION

Anthocyanins, a group of phenolic compounds widely found in the plant kingdom, are responsible for the orange, red, violet, and blue colors observed in nature (*1*). The color quality of fresh and processed fruits and vegetables, together with documented health benefits, has led to renewed interest in these pigments as part of our diet (*1*,*2*). Because the pigments are not stable, they tend to be decolorized or degraded during processing and storage (*3*). The decolorization and degradation induced the chemical transformation and affected the performance and biological activity of anthocyanin-containing food. Therefore, knowledge was required to understand the mechanism of anthocyanin degradation exposed to different conditions. It is well-known that temperature, oxygen, and the pH value of medium are the most important factors causing degradation of anthocyanins (*4*).

In aqueous solutions, common anthocyanins exist as a mixture of flavylium cation (AH^+, red), quinonoidal anhydrobase (A, blue), carbinol pseudobase (B, colorless), and chalcone (C, colorless or yellow) in chemical equilibrium (*4*). The color and stability of the anthocyanins depend on these three equilibria. Changes of conditions break the equilibria and lead to degradation of the anthocyanins (*4*). The acid−base equilibrium is broken down with rising temperature, which accelerates the AH^+ to form chalcone and then other products. Seeram et al. (*3*) investigated the degradation products of cyanidin-3-glucosylrutinoside, cyanidin-3-rutinoside, and cyanidin-3-glucoside under heat and identified the degradation products as cyanidin-3-glucoside, cyanidin, protocatechuic acid, 2,4-dihydroxybenzoic acid, and 2,4,6-trihydroxybenzoic acid. Their results indicated that under pH 3 and 100 °C, hydrolysis of the glycosidic bond was the first step in the degradation of cyanidin-3-glucosylrutinoside and cyanidin-3-rutinoside to form cyanidin-3-glucoside and then cyanidin. Furthermore, cyanidin proceeded through a highly unstable α-diketone intermediate to eventually form aldehydes and benzoic acid derivatives. Sadilova et al. (*5*) put forward a scheme of the predominant degradation pathways of cyanidin-3-glucoside, which is shown in **Figure 1**. Adams (*6*) found chalcone or α-diketone and cyanidin as thermal degradation products of cyanidin-3-glycosides under N_2 at 100 °C for 5 h. Sadilova et al. (*7*) identified chalcone glycoside, 4-hydroxybenzoic acid, protocatechuic acid, and phloroglucinaldehyde as the thermal degradation products of anthocyanins in elderberry and strawberry during heating at 95 °C and pH 3.5. Hrazdina and Franzese (*8*) studied the oxidation products of anthocyanidin-3,5-diglucosides under acidic and neutral conditions. Heated in neutral solutions with pH ranging from 6 to 7, malvidin-3,5-diglucoside degraded to 3,5-di(*O*-β-D-glucosyl)-7-hydroxycoumarin, but in acidic conditions, pH ranging from 1 to 3, malvidin-3,5-diglucoside degraded to the B-ring acid, the sugar substitute of 3-position, and 2,4,6-trihydroxyphenylacetic acid. Protocatechuic acid and 4,6-dihydroxy-2-*O*-β-D-glucosyl-3-oxo-2,

*Corresponding author (telephone 86-10-62737434-602; fax 86-10-62737434-604; e-mail liaoxjun@hotmail.com).

 Published on Web 02/17/2010

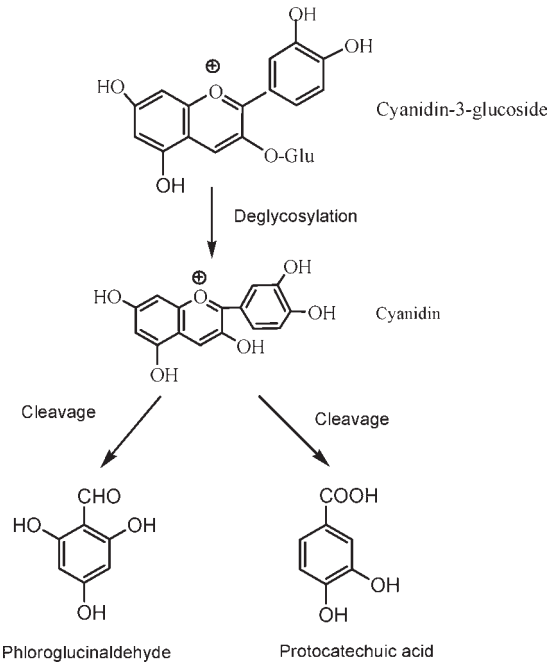

Figure 1. Scheme of the predominant thermal degradation pathways of Cyd-3-glc at pH 1 adapted from ref *7*.

3-dihydrobenzofuran have been reported as the oxidation products of cyanidin-3-glucoside (*9*, *10*). Enzymatic action has also been implicated in the degradation of anthocyanins. Polyphenol oxidase catalyzes the reaction between anthocyanin and the oxidated products of polyphenol (*11*). Anthocyanase may hydrolyze the glycosidic bonds of anthocyanins to yield much more unstable anthocyanidins, which undergo spontaneous decolorization and degradation (*12*). Glucosidase catalyzes the hydrolysis of the glycosidic bond of the anthocyanins at C_3 and C_5 to yield much more unstable anthocyanidins, which undergo spontaneous degradation (*4*). Moreover, the metabolism of anthocyanins by the intestinal microflora was investigated by Keppler and Humpf (*13*). It was proved that the microflora has an enormous hydrolytic potential and even ring scission properties. Glycosidic bonds in anthocyanins are cleaved by bacteria. Protocatechuic acid was detected in vivo as a degradation product of cyanidin-3-glucoside after oral ingestion (*10*). On the basis of the results of these investigations, it was postulated that anthocyanins degraded by either of two pathways. One was the hydrolysis of anthocyanins, which caused the loss of glycosyl moieties to form aglycone, followed by the formation of a more unstable α-diketone, and then the final products including aldehydes and benzoic acid derivatives. Another was pseudobase formation as the first step in the process, and then chalcones and coumarin glycosides, and the chalcones would undergo a further degradation. To date, the degradation mechanism of anthocyanins has not been fully elucidated under different conditions.

PEF is a novel nonthermal processing technology and is an alternative preservation method for thermal treatment (*14*). It is applied to inactivate microorganisms and enzymes in foods for improving shelf-life stability (*15*) and offers better retention of color than thermal processes (*16*). However, Zhang et al. (*17*) found that PEF induced the degradation of Cyd-3-glc, and the degradation rate constant is 10^3 times higher than that of thermal degradation. Odriozola-Serrano et al. (*18*) reported that the pulse polarity and frequency of pulsed electric fields had significant effect on the retention of anthocyanins in strawberry juices. In another investigation, the degradation rate constant of anthocyanins in strawberry juice exposed to high-intensity pulsed electric field (*18*) was calculated, and it was far greater than those for samples exposed at a lower electric field strength of 1.2, 2.2, or 3.0 kV/cm. However, few investigations showed the anthocyanin degradation products and the formation kinetics by PEF. The objective of this investigation was to analyze the effect of PEF on Cyd-3-glc degradation and to identify its degradation products.

MATERIALS AND METHODS

Chemicals. Cyd-3-glc (Kuromanin, HPLC grade) was purchased from Extrasynthèse (Genay, France). Protocatechuic acid, 2,4-dihydroxybenzoic acid, 2,4,6-trihydroxybenzoic acid, and formic acid (99% of purity) were obtained from Sigma-Aldrich Chemicals (St. Louis, MO). Methanol (HPLC grade) used in HPLC/ESI-MS and HPLC was obtained from Fisher Chemicals Co., Inc. (Waltham, MA). Other solvents were purchased from Beijing Chemical Reagent Co. (Beijing, China).

PEF Treatment. Cyd-3-glc reference compound (1.5 mg) was dissolved in a 30% methanol solution, which contained 2.1% formic acid (pH 1.7). The concentration of Cyd-3-glc was 3.340×10^{-4} mol/L. PEF treatment was performed by using a laboratory scale pulse generator system (*17*), which consisted of a high-voltage pulse generator, a high-voltage pulse treatment chamber, a peristaltic pump, and stainless steel parallel-plate electrodes. Main parameters were exponentially decaying wave, 300 μs pulse duration, 1 Hz pulse frequency, 0.5 μF capacitor, and 2 mL treatment chamber. The gap between the high-voltage electrode and the ground electrode was 0.5 cm. The high voltage was monitored by a Trek oscilloscope (Tektronix TDS 210, Tektronix, Beaverton, OR). Besides, a thermocouple was attached to the exit of the chamber to monitor the post-treatment temperature.

Furthermore, to avoid contamination of the foreign matters in the system, the circulation path of samples, including the stainless steel treatment chamber, silicon tube, and sample bottle, was washed with HPLC grade methanol before use. Twenty milliliter of Cyd-3-glc solution was injected into the sample bottle, which was not sealed; then, the solution was cycled in the circulation path by peristaltic pump and, thereafter, PEF treatment was carried out until the desired treatment time was reached. Particularly, the total PEF treatment time was calculated as $t = \frac{V_2}{V_1} \times n \times F \times \delta$, t is treatment time, V_1 is the total volume of treated sample (mL), V_2 is the volume of the treatment chamber (mL), n is the pulse number, F is pulse frequency (Hz), and δ is pulse width (μs). The sample for spectral and kinetics analysis was subjected to electric strengths of 7, 14, and 22 kV/cm for 1.8×10^{-3}, 3.6×10^{-3}, 5.4×10^{-3}, and 7.2×10^{-3} s, respectively. The sample for the identification of degradation product was performed at the highest electric strength of 22 kV/cm for 9.0×10^{-3} s to obtain enough degradation product. During performance, the sample bottle was immersed in ice water all the time to ensure the temperature of the treated samples was < 55 °C by the thermocouple. Similarly, Cyd-3-glc was heated at 95 °C for 12 and 24 h by water bath for more degradation products and then cooled by ice water immediately.

Spectral Analysis. Spectra of PEF or thermally treated Cyd-3-glc were recorded on a UV spectrophotometer (Cary 50, Varian Co.) at ambient temperature, by using 1 cm path length quartz cells. The scanning wavelength ranged from 190 to 800 nm in steps of 1.00 nm.

HPLC-PDA Analysis. The quantification of Cyd-3-glc and its degradation products was detected by using HPLC-PDA. The HPLC system consists of a Shimadzu (Kyoto, Japan) liquid chromatography system equipped with an LC-10AT pump, a model SPD-M10A photodiode array detector, and a model SCL-10A communications bus module. One milliliter of sample was filtered through 0.22 μm and analyzed on a Cosmosil $5C_{18}$-RA-II column (250 mm × 4.6 mm i.d., 5 μm, Cosmosil, Kyoto, Japan) at a column temperature of 35 °C. The process of chromatographic separation was as follows: Mobile phase B was a mixture of formic acid, water, and HPLC grade methanol in a ratio of 1:4:5 (v/v/v). Mobile phase A was water containing 1% formic acid. The separation of Cyd-3-glc and its degradation product was achieved within 48 min; the first 2 min was performed isocratically with 12% B at 0.8 mL/min, followed by a linear gradient from 12 to 60% B in 28 min at 0.8 mL/min, then from 60 to 100% B in 18 min at 0.3 mL/min. The volume of injection was 20 μL.

Besides, Cyd-3-glc was detected at 519 nm and the degradation products were detected at 280 nm using a PDA detector (Shimadzu, Japan). Concentration of Cyd-3-glc and its degradation product was expressed by using corresponding peak area. Meanwhile, the UV−vis absorption spectra of Cyd-3-glc degradation products were recorded online during HPLC analysis, and spectral measurements were taken over the wavelength range of 190−800 nm in steps of 2 nm.

HPLC-ESI-MS Analysis. The identification of Cyd-3-glc degradation products was performed by using HPLC-ESI-MS (Agilent 1100 MSD series) system, with a UV−vis detector coupled to a mass spectrometer (ion trap analyzer) equipped with an ESI interface. The separation process was performed as described above. In this system, MS parameters were as follows: capillary voltage, 3500 V; detector voltage, 3500 V; drying gas temperature, 350 °C; gas flow (N_2), 10 mL/min. The instrument was operated in negative ion mode scanning from m/z 100 to 1000 at a scanning rate of 1.47 s/cycle.

Kinetics Analysis. The degradation of Cyd-3-glc and the formation of its degradation product were subjected to regression analysis by using the first-order model

$$\ln(C_t/C_0) = -k_c t$$

$$\ln(Q_t/Q_0) = -k_Q t$$

where C_t, C_0, Q_t, and Q_0 were the concentrations of Cyd-3-glc and its degradation product at times t and t_0, respectively. k was the reaction rate constant (s^{-1}), and t was the treatment time (s). Moreover, the Z_E value indicating the electric field sensitivity of Cyd-3-glc was obtained using procedures analogous to that employed in thermal degradation kinetics studies by plotting the logarithm of k_2/k_1 versus the intensity of the electric field. Mathematically, it followed the equation

$$\ln\left(\frac{k_{c2}}{k_{c1}}\right) = \frac{E_{c2} - E_{c1}}{Z_E}$$

Data Analysis. All experiments were performed in triplicates. The statistical analysis of experimental results was based on analysis of variance. Significant difference was statistically considered at the level of $P < 0.05$. The analysis was performed with SAS, version 9.0 (SAS Institute Inc., Cary, NC).

RESULTS AND DISCUSSION

UV−Vis Spectral Alteration of Cyd-3-glc Exposed to PEF. The UV−vis spectra of Cyd-3-glc in an aqueous solution exposed to PEF as a function of the electric field strength or treatment time are shown in **Figure 2**. PEF-treated Cyd-3-glc exhibited spectral characteristics similar to the control Cyd-3-glc. The spectra were characterized by two sharp peaks at 280 and 519 nm and two shoulders around 333 and 440 nm. These spectral characteristics for Cyd-3-glc were previously reported by Fossen et al. (*19*) and Gao et al. (*20*). In an acidic solution, Cyd-3-glc is present as a mixture of flavylium cation (AH^+, red), quinonoidal anhydrobase (A, blue), carbinol pseudobase (B, colorless), and chalcone (C, colorless or yellow) (*4*). The peaks at 280 and 519 nm are the characteristic absorption of the cation form of the flavylium structure (*20*). The shoulder peak at 440 nm is identified as browning compounds (*19*, *20*), and 333 nm is a characteristic absorption of chalcone (*4*, *6*). **Figure 2** also shows a significant alteration in the spectral intensity of Cyd-3-glc exposed to PEF. With increasing electric field strength for a treatment time of 7.2×10^{-3} s or the treatment time at electric field strength of 22 kV/cm, both the peak intensity at 280 and 519 nm and the shoulder intensity at 440 nm decreased, but the shoulder intensity at 333 nm increased. These observations indicated that PEF caused the degradation of Cyd-3-glc and resulted in an UV−vis spectral alteration.

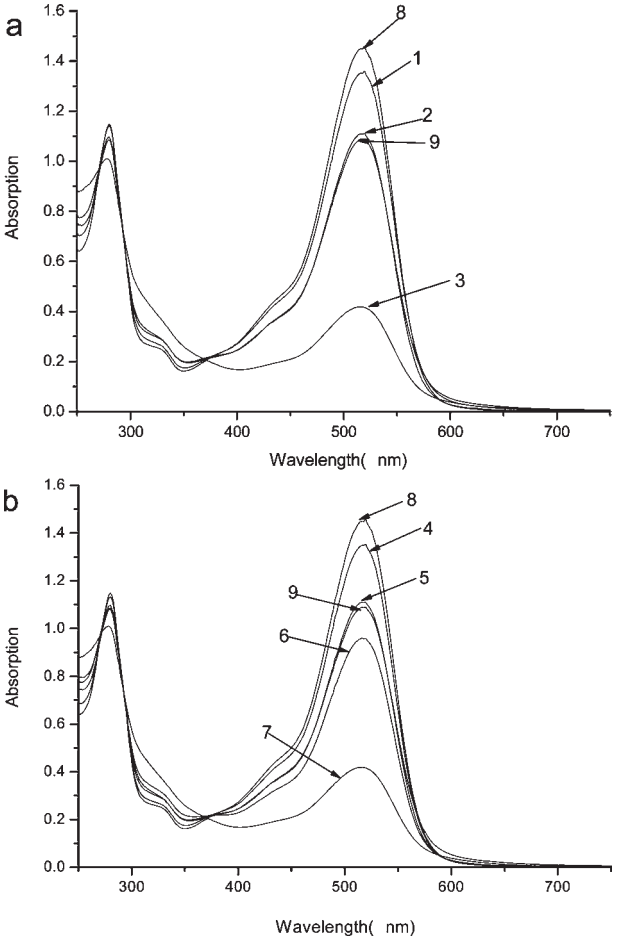

Figure 2. UV−vis spectra alteration of Cyd-3-glc solution exposed to PEF: (**a**) at (1) 7, (2) 14, and (3) 22 kV/cm for 7.2×10^{-3} s; (**b**) at 22 kV/cm for (4) 1.8×10^{-3}, (5) 3.6×10^{-3}, (6) 5.4×10^{-3}, and (7) 7.2×10^{-3} s. The others were (8) control and (9) thermal treatment at 95 °C for 12 h.

Identification of Cyd-3-glc Degradation Products Exposed to PEF. The degradation products of Cyd-3-glc exposed to PEF were detected at 280 and 519 nm by using a HPLC-PDA method. As shown in **Figure 3**, the HPLC chromatographs indicated that Cyd-3-glc degraded significantly after PEF or thermal treatment. As a control Cyd-3-glc, there was only one peak at 519 nm with a retention time of 11.28 min representing Cyd-3-glc in **Figure 3a**, which was designated compound **8**. A new peak with a retention time of 25.85 min at 519 nm appeared in thermally treated Cyd-3-glc in **Figure 3b**, which was designated compound **13**, suggesting that the thermal treatment induced a new compound formation, but this new peak was absent in PEF-treated Cyd-3-glc as shown in **Figure 3c**. Furthermore, the HPLC profile of PEF or thermally treated Cyd-3-glc at 280 nm is shown in **Figure 4**. Similarly, there was only one peak at 280 nm representing Cyd-3-glc in the control Cyd-3-glc. However, more new peaks at 280 nm were observed for PEF or thermally treated Cyd-3-glc, indicating that PEF or thermal treatment induced a formation of new compounds at 280 nm. All of these peaks were designated compounds **1**, **2**, **3**, **4**, **6**, **7**, **11**, and **12** in PEF or thermally treated Cyd-3-glc in **Figure 4**, respectively. Compound **10** was present in only PEF treated Cyd-3-glc, whereas compounds **5**, **9**, and **13** were present in only thermally treated Cyd-3-glc, indicating that the degradation products of Cyd-3-glc exposed to PEF and thermal treatment were different. The discrepancy in degradation products implied that the

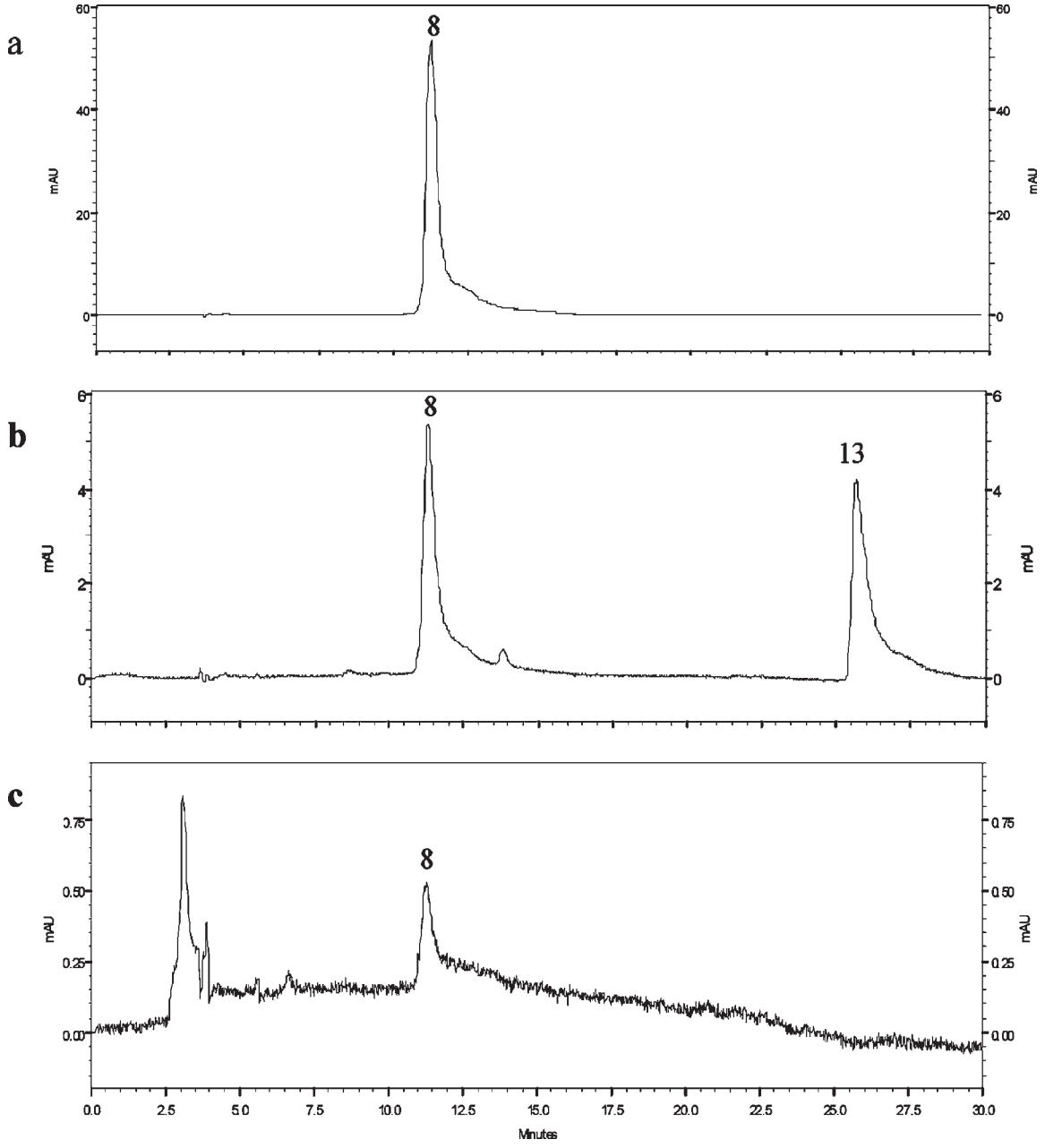

Figure 3. HPLC chromatograms of Cyd-3-glc recorded at 519 nm: (**a**) untreated as control; (**b**) thermal treatment at 95 °C for 24 h; (**c**) PEF treatment at 22 kV/cm for 9.0×10^{-3} s.

degradation pathways of Cyd-3-glc induced by PEF and thermal treatments could be different.

On the basis of these observations, the degradation products of Cyd-3-glc were identified by using a combination of HPLC, UV−vis spectra, and HPLC-ESI-MS as shown in **Table 1**. Compound **4** had a retention time of 7.19 min and a maximum absorption wavelength (λ_{max}) of 266 nm. Its molecular ion (M^+) m/z 152.7 was assigned to protocatechuic acid, generating a typical fragment at m/z 108.8. All of this spectral information was in agreement with the reference compound of protocatechuic acid. As a matter of fact, protocatechuic acid was found to be a common degradation product of anthocyanins in earlier investigations. As described by Seeram et al. (*3*), protocatechuic acid was regarded as one thermal degradation product of cyanidin-3-glucosylrutinoside, cyanidin-3-rutinoside, and cyanidin-3-glucoside resulting from the hydrolysis of glycosidic bond by thermal treatment. In addition, Keppler and Humpf (*13*) also reported protocatechuic acid as a hydrolysis product of the aglycone cyanidin by the intestinal microflora. Sadilova et al. (*7*) monitored protocatechuic acid as a thermal degradation product of anthocyanins from strawberry and black carrot due to the hydrolysis by heating, and protocatechuic acid was considered to be the remainder of the B-ring. Moreover, protocatechuic acid was identified as the oxidation product of anthocyanins (*8*, *9*).

Compound **7** had a retention time of 10.81 min and two maximum absorption wavelengths (λ_{max}) of 244 and 280 nm shown in **Figure 5**, which were similar to those of the authentic compound 2,4,6-trihydroxybenzoic acid (phloroglucinol acid). Compound **7** also was analyzed by HPLC-ESI-MS, but the signal of 2,4,6-trihydroxybenzoic acid was not found, which was attributed to the lower signal response for MS detector. It was assumed that compound **7** was possibly 2,4,6-trihydroxybenzoic acid, but a further study should be done to confirm. In accordance with

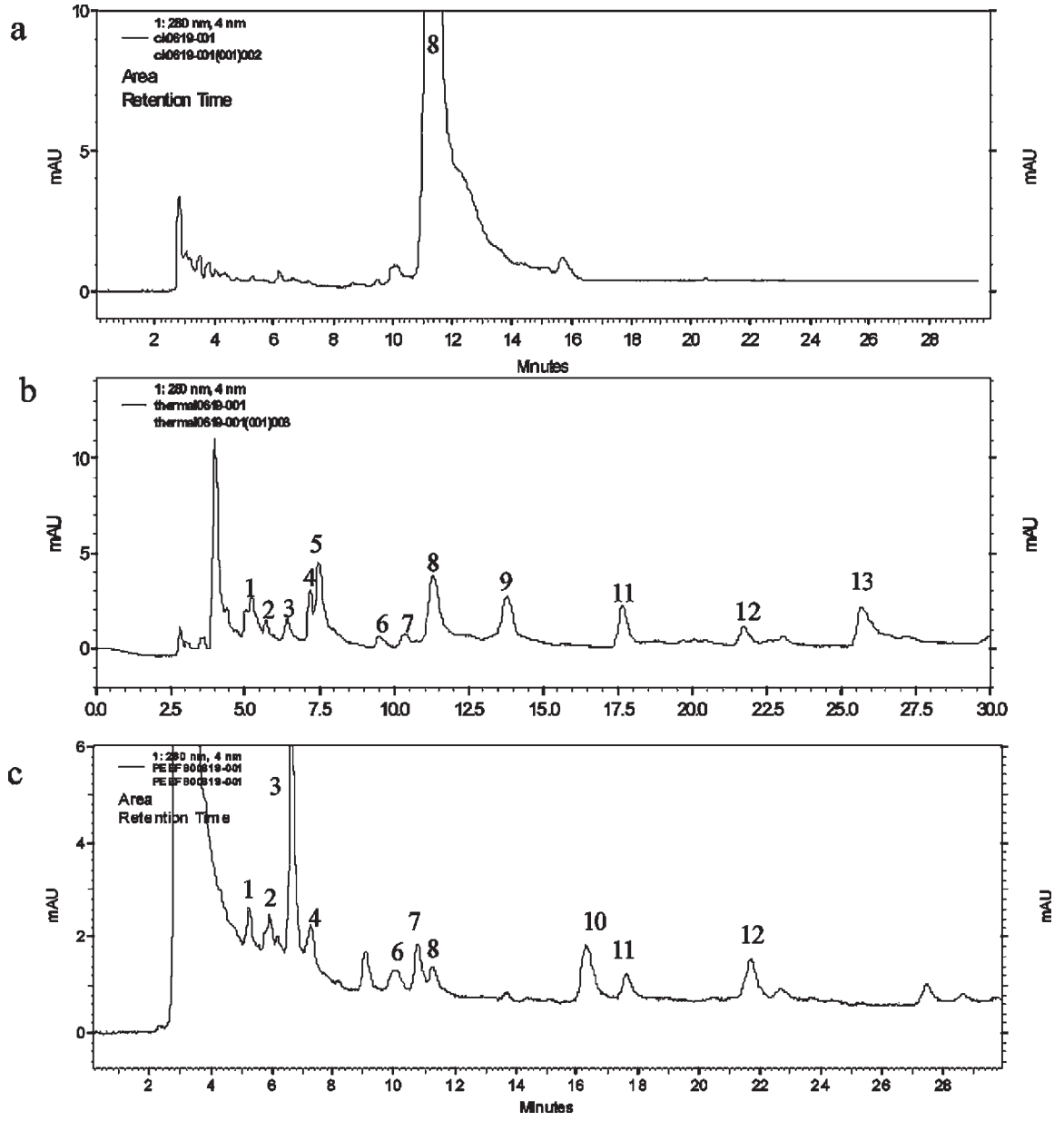

Figure 4. HPLC chromatograms of Cyd-3-glc recorded at 280 nm: (**a**) untreated as control; (**b**) thermal treatment at 95 °C for 24 h; (**c**) PEF treatment at 22 kV/cm for 9.0×10^{-3} s.

Table 1. HPLC, UV−Vis, and MS Spectral Data of the Degradation Products of Cyd-3-glc Induced by PEF at 22 kV/cm for 9.0×10^{-3} s and Thermal Treatment at 95 °C for 24 h

no.	retention time (min)	present in PEF or thermal treatment	HPLC-PDA	HPLC-MS	compound
1	5.22	PEF and thermal	274, 316	a	b
2	5.91	PEF and thermal	268	a	b
3	6.65	PEF and thermal	276	a	b
4	7.19	PEF and thermal	266	152.7, 108.8	protocatechuic acid
5	7.49	only thermal	284, 328	a	b
6	9.98	PEF and thermal	244, 302	a	b
7	10.81	PEF and thermal	244, 280	a	2,4,6-trihydroxybenzoic acid
8	11.28	PEF and thermal	280, 519	449, 287	Cyd-3-glc
9	13.7	only thermal	250, 286, 322	a	b
10	16.32	only PEF	245, 276, 308	a	b
11	17.67	PEF and thermal	244, 278	a	b
12	21.69	PEF and thermal	244, 278	a	b
13	25.85	only thermal	280, 525	286.8	cyanidin

[a] Not determined. [b] Not identified.

previous findings (*7*, *13*), the A-ring of the anthocyanin was degraded to phloroglucinol aldehyde, which was further oxidized into phloroglucinol acid. Seeram et al. (*3*) found that phloroglucinol acid also was one of the thermal degradation products of

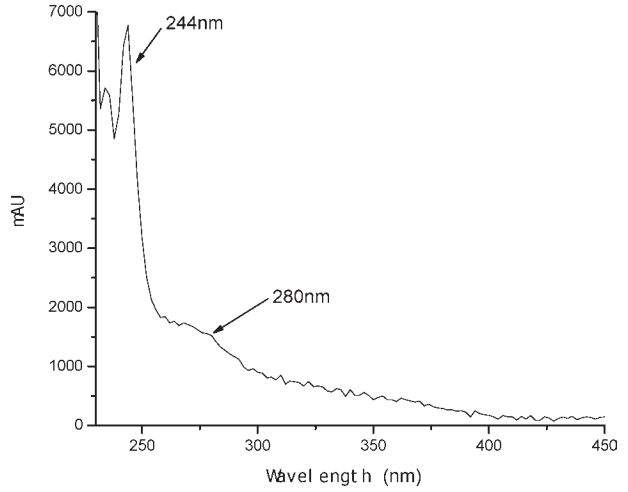

Figure 5. UV−vis spectrum of compound **7**.

cyanidin-3-glucosylrutinoside, cyanidin-3-rutinoside, and cyanidin-3-glucoside.

Compound **13** was present in only thermally treated Cyd-3-glc with a retention time of 25.85 min and two maximum absorption wavelengths λ_{max} at 280 and 525 nm. An M^+ at m/z 286.7 was found in the mass spectrum of compound **13**, which well matched with the previously reported spectrum of cyanidin (*21*, *22*). Thus, compound **13** was identified as cyanidin, confirming that the hydrolysis of the glycosidic moiety and aglycon formation were the initial reactions in thermally treated Cyd-3-glc; this finding was consistent with earlier investigations (*3*, *5*). However, compound **13** was absent in PEF-treated Cyd-3-glc. To confirm the absence of cyanidin, PEF treated Cyd-3-glcs at 1.2, 2.2, and 3.0 kV/cm for 1.8×10^{-3}, 3.6×10^{-3}, 5.4×10^{-3}, and 7.2×10^{-3} s were also injected. Cyanidin could not be detected in any of the PEF treated Cyd-3-glc solutions. To sum up, it can be confirmed that cyanidin was absent in PEF treated Cyd-3-glc. Unfortunately, other compounds from PEF treated Cyd-3-glc in the HPLC profile at 280 nm could not be identified in this investigation.

Kinetics of Cyd-3-glc Degradation and Protocatechuic Acid Formation Exposed to PEF. The degradation kinetics of Cyd-3-glc exposed to PEF at electric field strength from 7 to 22 kV/cm is shown in **Figure 6a**, which was well fitted to a first-order reaction; the kinetic parameters are shown in **Table 2**. All of the regression coefficients R^2 for a given electric field upon the electric field strength were >0.96, indicating an excellent correlation between Cyd-3-glc degradation and treatment time. As the electric field intensity increased from 7 to 22 kV/cm, the degradation rate constants of Cyd-3-glc (k_c) increased from 25.72 to 166.00 s^{-1}. They were far greater than those in a lower electric field strength of ≤3 kV/cm (*17*). Besides, the degradation rate constants of Cyd-3-glc also were far greater than those in an electric field strength of 20−35 kV/cm using 1 μs square-wave bipolar pulses at 232 Hz (*18*). Differences in degradation rate constant resulting from PEF treatments were attributed not only to factors that were intrinsic to the food matrix but also to other factors including PEF system, pulse characteristics, and electrical conditions (*18*, *23*). Additionally, the electric field sensitivity of Cyd-3-glc degradation could be expressed by the parameter Z_E. The Z_E value was generally obtained as the reciprocal slopes of regression plots of logarithms of k values versus electric field strength. Logarithms of k values of Cyd-3-glc degradation had good linear relationships with the electric field strength, and the regression coefficient R^2 was 0.97. The Z_E value of Cyd-3-glc degradation obtained from the slopes was 8.10 kV/cm. **Figure 6b** shows the formation of protocatechuic acid after PEF treatment. Protocatechuic acid increased significantly with increasing electric intensity and treatment time ($P < 0.05$). The result was not in agreement with that documented by Zhao et al. (*24*), who found no degradation of polyphenols and catechins in tea during PEF treatment. We believed that the difference was attributed to the pulse waves of PEF used in both experiments. The kinetics of protocatechuic acid formation also was well fitted to a first-order reaction as a function of the electric field strength apart from at 7.0 kV/cm as shown in **Table 2**. Moreover, a perfect correlation between Cyd-3-glc degradation and protocatechuic acid formation at higher electric field strength, >7.0 kV/cm, is displayed in **Figure 7**. Cyd-3-glc degradation and protocatechuic acid formation were closely correlated to the electric field strength or treatment time of PEF.

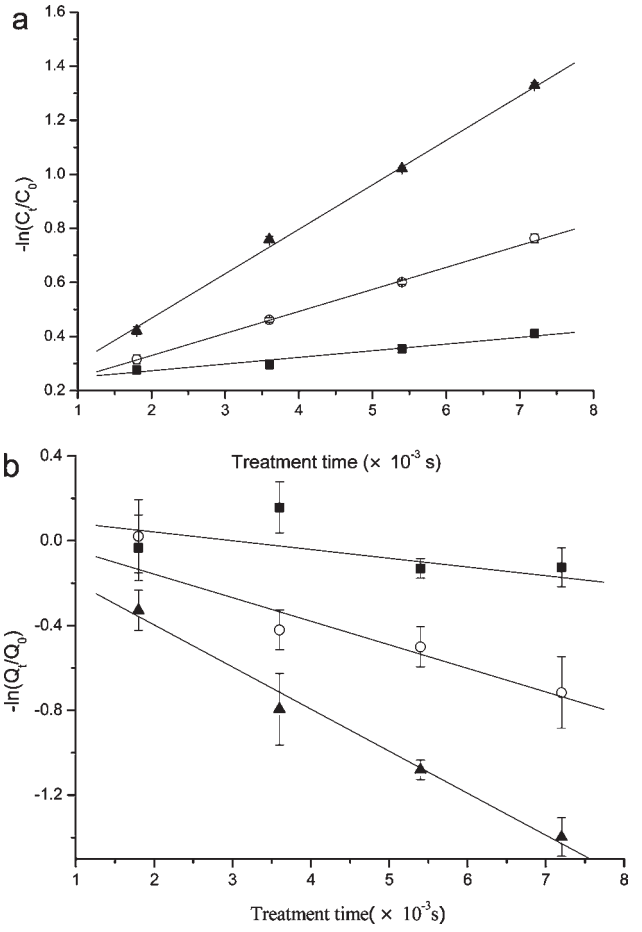

Figure 6. Kinetics of (**a**) Cyd-3-glc degradation and (**b**) protocatechuic acid formation after PEF treatment as a function of treatment time at (■) 7 kV/cm, (○) 14 kV/cm, and (▲) 22 kV/cm of the electric field strength.

Table 2. Kinetic Parameters of the Degradation of Cyd-3-glc and the Formation of Protocatechuic Acid after PEF Treatment

	Cyd-3-glc		protocatechuic acid		
electric field strength (kV/cm)	k_c (s^{-1})	R^2	k_Q (s^{-1})	R^2	correlation coefficient
7	25.72	0.9979	−31.36	0.2932	−0.4626
14	82.33	0.9991	−127.30	0.9126	−0.9638
22	166.00	0.9630	−194.13	0.9873	−0.9480

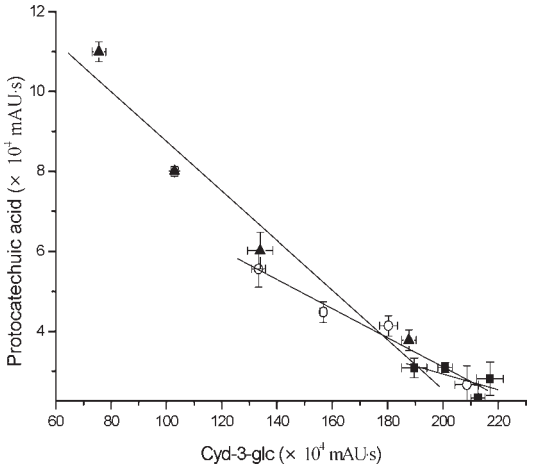

Figure 7. Correlation between the degradation of Cyd-3-glc and the formation of protocatechuic acid exposed to PEF at (■) 7, (○) 14 kV/cm, and (▲) 22 kV/cm of the electric field strength.

Possible Mechanism of Cyd-3-glc Exposed to PEF. The absence of cyanidin in PEF treated samples indicated that the first step of Cyd-3-glc degradation induced by PEF was not the hydrolysis of a glycosidic bond. According to previous reports, PEF could induce electrochemical reactions and lead to changes of temperature, pH, and chemical composition (*25*−*27*): for example, the release of Fe^{2+}/Fe^{3+} from stainless steel electrodes (*25*, *28*), the increase of oxygen dissolution (*27*), and even the presence of hydrogen peroxide caused by a lower pH value of sample solution (*29*). These may be the possible reasons resulting in the absence of cyanidin in PEF treated sample. In the investigation of Tsuda et al. (*9*), the oxidation products of cyanidin 3-*O*-*β*-D-glucoside with 2,2′-azobis(2,4-dimethylvaleronitrile) were identified as 4,6-dihydroxy-2-*O*-*β*-D-glucosyl-3-oxo-2,3-dihydrobenzofuran and protocatechuic acid. According to Hrazdina and Franzesè's (*8*) investigation, upon nucleophilic attack of the H_2O_2 at the 2-carbon of the molecule, the heterocyclic ring was cleaved between C_2 and C_3 to form *o*-benzoyloxyphenylacetic acid esters of the malvone type. These esters were further hydrolyzed under alkaline conditions to the B-ring acid, the sugar substituent of the 3-position, and the elusive 2,4,6-trihydroxyphenylacetic acid (*8*). The results mentioned above indicated that cyanidin could be absent in the oxidized reaction of anthocyanin. Oxidation could thus play an important role in the degradation of Cyd-3-glc exposed to PEF. Moreover, great changes in pH in the vicinity of electrodes (the acidification around the anode and alkalization at the cathode) will break down the chemical equilibrium of the Cyd-3-glc solution and directly lead to the formation of quinonoidal anhydrobase or carbinol pseudobase, which was unstable and further degraded to chalcones and coumarin glycosides.

LITERATURE CITED

(1) Mazza, G.; Miniati, E. *Anthocyanins in Fruits, Vegetables, And Grains*; CRC Press: Boca Raton, FL, 1993.
(2) Bridle, P.; Timberlake, C. F. Anthocyanins as natural food colours-selected aspects. *Food Chem.* **1997**, *58*, 103–109.
(3) Seeram, N. P.; Bourquin, L. D.; Nair, M. G. Degradation products of cyanidin glycosides from tart cherries and their bioactivities. *J. Agric. Food Chem.* **2001**, *49*, 4924–4929.
(4) Markakis, P. *Anthocyanins as Food Colors*; Academic Press: New York, 1982; pp 163−180.
(5) Sadilova, E.; Stintzing, F. C.; Carle, R. Thermal degradation of acylated and non-acylated anthocyanins. *J. Food Sci.* **2006**, *71* (8), 504–512.
(6) Adams, J. B. Thermal degradation of anthocyanins with particular reference to the 3-glycosides of cyanidin I. In acidified aqueous solution at 100°C. *J. Sci. Food Agric.* **1973**, *24*, 747–762.
(7) Sadilova, E.; Carle, R.; Stintzing, F. C. Thermal degradation of anthocyanins and its impact on color and in vitro antioxidant capacity. *Mol. Nutr. Food Res.* **2007**, *51*, 1461–1471.
(8) Hrazdina, G.; Franzese, A. J. Oxidation products of acylated anthocyanins under acidic and neutral conditions. *Phytochemistry* **1974**, *13*, 231–234.
(9) Tsuda, T.; Ohshima, K.; Kawakishi, S.; Osawa, T. Oxidation products of cyanidin 3-*O*-*β*-D-glucoside with a free radical initiator. *Lipids* **1996**, *31* (2), 1259–1263.
(10) Tsuda, T.; Horio, F.; Osawa, T. Absorption and metabolism of cyanidin-3-*O*-*β*-D-glucoside in rats. *FEBS Lett.* **1999**, *449*, 179–182.
(11) Kader, F.; Haluk, J. P.; Nicolas, J. P.; Metche, M. Degradation of cyanidin-3-glucoside by blueberry polyphenol oxidase: kinetics study and mechanisms. *J. Agric. Food Chem.* **1998**, *46*, 3060–3065.
(12) Jiang, Y. M.; Duan, X. U.; Joyce, D.; Zhang, Z. Q.; Li, J. R. Advances in understanding of enzymatic browning in harvested litchi fruit. *Food Chem.* **2004**, *88*, 443–446.
(13) Keppler, K.; Humpf, H. Metabolism of anthocyanins and their phenolic degradation products by the intestinal microflora. *Bioorg. Med. Chem.* **2005**, *13*, 5195–5205.
(14) Zhong, K.; Chen, F.; Wang, Z. F.; Wu, J. H.; Liao, X. J.; Hu, X. S. Inactivation and kinetic model for the *Escherichia coli* treated by a co-axial pulsed electric field. *Eur. Food Res. Technol.* **2005**, *221*, 472–478.
(15) Vega-Mercado, H.; Martín-Belloso, O.; Qin, B. L.; Chang, F. J.; Góngora-Nieto, M. M.; Barbosa-Cánovas, G. V.; Swanson, B. G. Non-thermal food preservation: pulsed electric fields. *Trends Food Sci. Technol.* **1997**, *8*, 151–157.
(16) Hye, W. Y.; Streaker, C. B.; Zhang, Q. H.; Min, D. B. Effects of pulsed electric fields on the quality of orange juice and comparison with heat pasteurization. *J. Agric. Food Chem.* **2000**, *48*, 4597–4605.
(17) Zhang, Y.; Liao, X. J.; Ni, Y. Y.; Wu, J. H.; Hu, X. S.; Wang, Z. F.; Chen, F. Kinetic analysis of the degradation and its color of cyanidin-3-glucoside exposed to pulsed electric field. *Eur. Food Res. Technol.* **2007**, *224*, 597–603.
(18) Odriozola-Serrano, I.; Soliva-Fortuny, R.; Gimeno-Aó, V.; Martín-Belloso, O. Kinetic study of anthocyanins, vitamin C, and antioxidant capacity in strawberry juices treated by high-intensity pulsed electric fields. *J. Agric. Food Chem.* **2008**, *56*, 8387–8393.
(19) Fossen, T.; Cabrita, L.; Andersen, Q. M. Colour and stability of pure anthocyanins influenced by pH including the alkaline region. *Food Chem.* **1998**, *63*, 435–440.
(20) Gao, L.; Girard, B.; Mazza, G.; Reynolds, A. G. Changes in anthocyanins and color characteristics of Pinot Noir wines during different vinification processes. *J. Agric. Food Chem.* **1997**, *45*, 2003–2008.
(21) Giusti, M. M.; Rodríguez-Saona, L. E.; Wrolstad, R. E. Molar absorptivity and color characteristics of acylated and non-acylated pelargonidin-based anthocyanins. *J. Agric. Food Chem.* **1999**, *47*, 4631–4637.
(22) Stintzing, F. C.; Stintzing, A. S.; Carle, R.; Frei, B.; Wrolstad, R. E. Color and antioxidant properties of cyanidin-based anthocyanin pigment. *J. Agric. Food Chem.* **2002**, *50*, 6172–6181.
(23) Odriozola-Serrano, I.; Soliva-Fortuny, R.; Martín-Belloso, O. Impact of high-intensity pulsed electric fields variables on vitamin C, anthocyanins and antioxidant capacity of strawberry juice. *LWT − Food Sci. Technol.* **2009**, *42* (1), 93–100.
(24) Zhao, W.; Yang, R. J; Wang, M.; Lu, R. R. Effects of pulsed electric fields on bioactive components, colour and flavour of green tea infusions. *Int. J. Food Sci. Technol.* **2009**, *312* (44), 312–321.
(25) Loomis-Husselbee, J. W.; Cullen, P. J.; Irvine, R. F.; Dawson, A. P. Electroporation can cause artifacts due to solubilization of cations from the electrode plates. *Biochem. J.* **1991**, *277*, 883–885.

(26) Saulis, G.; Lapė, R.; Pranevičiūtė, R.; Mickevičius, D. Changes of the solution pH due to exposure by high-voltage electric pulses. *Bioelectrochemistry* **2005**, *67*, 101–108.
(27) Rajeshwar, K.; Ibanez, J. G.; Swain, G. M. Electrochemistry and the environment. *J. Appl. Electrochem.* **1994**, *24* (11), 1077–1091.
(28) Roodenburg, B.; Morren, J.; Berg, H. E. (Iekje); de Haan, Sjoerd, W. H. Metal release in a stainless steel pulsed electric field (PEF) system: part II. The treatment of orange juice; related to legislation and treatment chamber lifetime. *Innovative Food Sci. Emerging Technol.* **2005**, *6*, 337–345.
(29) Zi, Z.; Zeng, X. A.; Hou, Y.; Liu, Y. Y. Change and reaction of dissolved oxygen under the treatment of pulsed electric fields. *High Voltage Eng.* (*Chinese*) **2008**, *34* (4), 695–699.

Received for review June 11, 2009. Revised manuscript received February 5, 2010. Accepted February 7, 2010. This research work is supported by the National Natural Science Foundation of China (No. 30771511), The National High Technology Development Project of China (No. 2007AA100405 and 2007AA100404), and China Agricultural University Research Fund (No. 2007051).